

## Fermion-Parity Anomaly of the Critical Supercurrent in the Quantum Spin-Hall Effect

C. W. J. Beenakker,<sup>1</sup> D. I. Pikulin,<sup>1</sup> T. Hyart,<sup>1</sup> H. Schomerus,<sup>2</sup> and J. P. Dahlhaus<sup>1</sup>

<sup>1</sup>*Instituut-Lorentz, Universiteit Leiden, Post Office Box 9506, 2300 RA Leiden, The Netherlands*

<sup>2</sup>*Department of Physics, Lancaster University, Lancaster LA1 4YB, United Kingdom*

(Received 26 October 2012; published 2 January 2013)

The helical edge state of a quantum spin-Hall insulator can carry a supercurrent in equilibrium between two superconducting electrodes (separation  $L$ , coherence length  $\xi$ ). We calculate the maximum (critical) current  $I_c$  that can flow without dissipation along a single edge, going beyond the short-junction restriction  $L \ll \xi$  of earlier work, and find a dependence on the fermion parity of the ground state when  $L$  becomes larger than  $\xi$ . Fermion-parity conservation doubles the critical current in the low-temperature, long-junction limit, while for a short junction  $I_c$  is the same with or without parity constraints. This provides a phase-insensitive, dc signature of the  $4\pi$ -periodic Josephson effect.

DOI: [10.1103/PhysRevLett.110.017003](https://doi.org/10.1103/PhysRevLett.110.017003)

PACS numbers: 74.45.+c, 71.10.Pm, 74.78.Fk, 74.78.Na

The quantum Hall effect and quantum spin-Hall effect both refer to a two-dimensional semiconductor with an insulating bulk and a conducting edge, and both exhibit a quantized electrical conductance between two metal electrodes. If the electrodes are superconducting, a current can flow in equilibrium, induced by a magnetic flux without any applied voltage. In the quantum Hall effect, the edge states are chiral (propagating in a single direction only) and two opposite edges are needed to carry a supercurrent [1–3]. Graphene is an ideal system to study this interplay of the Josephson effect and the quantum Hall effect in a strong magnetic field [4–6].

The interplay of the Josephson effect and the quantum spin-Hall effect, in zero magnetic field, has not yet been demonstrated experimentally but promises to be strikingly different [7]. The quantum spin-Hall insulator has helical edge states (propagating in both directions) that can carry a supercurrent along a single edge. The edge state couples a pair of Majorana zero modes, allowing for the transmission of unpaired electrons with  $h/e$  rather than  $h/2e$  periodic dependence on the magnetic flux [8,9].

An  $h/e$  flux periodicity corresponds to a  $4\pi$  periodicity in terms of the superconducting phase difference  $\phi$ , which means that the current-phase relationship has two branches  $I_{\pm}(\phi)$  and the system switches from one branch to the other when  $\phi$  is advanced by  $2\pi$  at a fixed total number  $\mathcal{N}$  of electrons in the system. This is referred to as a fermion-parity anomaly, because the two branches have different parity  $\sigma = \pm$  of the number of electrons in the superconducting ground state [8].

Josephson junctions come in two types [10], depending on whether the separation  $L$  of the superconducting electrodes is small or large compared to the coherence length  $\xi = \hbar v/\Delta$ , or equivalently, whether the superconducting gap  $\Delta$  is small or large compared to the Thouless energy  $E_T = \hbar v/L$ . Existing literature [7–9,11–18] has focused on the short-junction regime  $L \ll \xi$ . The supercurrent is then determined entirely by the phase dependence of a

small number of Andreev levels in the gap, just one per transverse mode. The phase dependence of the continuous spectrum above the gap can be neglected. As the ratio  $L/\xi$  increases, the Andreev levels proliferate and also the continuous spectrum starts to contribute to the supercurrent. Since  $\sigma$  is switched by changing the occupation of a single level, one might wonder whether a significant parity dependence remains in the long-junction regime.

Remarkably enough, the parity dependence becomes even stronger. While in a short junction the two branches  $I_+(\phi) = -I_-(\phi)$  differ only in sign, we find that in a long junction they differ both in sign and in magnitude. In particular, the largest current that can flow without dissipation is twice as large for  $I_-$  as it is for  $I_+$ . The difference is illustrated in Fig. 1, in the zero-temperature limit. The basic physics can be explained in simple terms, as we will do first, and then we will present a complete theory for a finite temperature and for an arbitrary ratio  $L/\xi$ .

We set the stage by summarizing the findings of Fu and Kane [7] in the short-junction regime. The spectrum of the Bogoliubov–de Gennes Hamiltonian  $H_{\text{BdG}}$  is a  $\pm\varepsilon$  symmetric combination of a discrete spectrum for  $|\varepsilon| < \Delta$  and a continuous spectrum for  $|\varepsilon| > \Delta$ . Since backscattering along the quantum spin-Hall edge is forbidden by time-reversal symmetry [19], this is a ballistic single-channel Josephson junction. In the limit  $L/\xi \rightarrow 0$  the discrete spectrum consists of a pair of levels at  $\varepsilon_{\pm} = \mp\Delta|\cos(\phi/2)|$ , while the continuous spectrum is  $\phi$  independent [20]. Quite generally, an eigenvalue  $\varepsilon(\phi)$  of  $H_{\text{BdG}}$  contributes to the supercurrent an amount

$$I(\phi) = \frac{ge}{\hbar} \frac{d}{d\phi} \varepsilon(\phi), \quad (1)$$

with  $g$  a factor that counts spin and other degeneracies [21]. There is no spin degeneracy at the quantum spin-Hall edge (since spin is tied to the direction of motion), so  $g = 1$  and the level  $\varepsilon_{\pm}$  contributes a supercurrent [7]

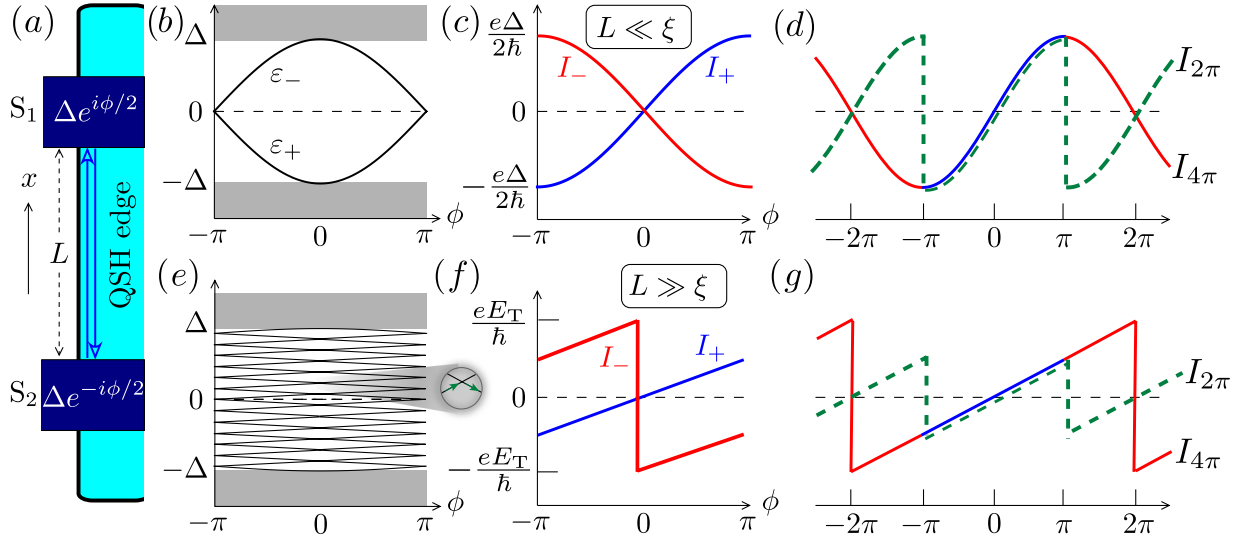


FIG. 1 (color online). Phase-dependent excitation spectrum of a Josephson junction along a quantum spin-Hall (QSH) edge (left panels) and corresponding zero-temperature supercurrent (right panels). The supercurrent  $I_{4\pi}$  is  $4\pi$ -periodic, with two branches  $I_+$  (blue solid),  $I_-$  (red solid) distinguished by the ground-state fermion parity and with a parity switch at  $\phi = \pm\pi$ . The top row shows the short-junction limit of Ref. [7], the bottom row the long-junction limit calculated here. (The jump in  $I_-$  at  $\phi = 0$  occurs because of the change in slope indicated by the green arrows in the magnified central part of the spectrum.) The  $2\pi$ -periodic supercurrent  $I_{2\pi}$  without parity constraints is also shown (green dashed). The critical current is the same for  $I_{4\pi}$  and  $I_{2\pi}$  in the short junction, but different by a factor of two in the long junction.

$$I_{\pm}(\phi) = \pm \frac{e\Delta}{2\hbar} \sin(\phi/2), \quad |\phi| < \pi. \quad (2)$$

To discuss the fermion-parity anomaly we assume, for definiteness, that the total number  $\mathcal{N}$  of electrons in the system is even. (A different choice amounts to a  $2\pi$  phase shift, or equivalently, an interchange of  $I_+$  and  $I_-$ .) The ground-state fermion parity  $\sigma$  is even for  $\phi = 0$  and switches to odd when  $\phi$  crosses  $\pi$ . Since  $\mathcal{N}$  is fixed, this topological phase transition must be accompanied by a switch between an even and odd number of quasiparticle excitations. At zero temperature, only the two levels  $\varepsilon_{\pm}$  closest to the Fermi level ( $\varepsilon = 0$ ) play a role, and the parity switch of  $\sigma$  means that a quasiparticle is transferred from  $\varepsilon_+ < 0$  to  $\varepsilon_- > 0$ . It cannot relax back from  $\varepsilon_-$  to  $\varepsilon_+$  at fixed parity of  $\mathcal{N}$ .

The resulting current-phase relationship can be represented by a switch between  $2\pi$ -periodic branches  $I_{\pm}(\phi)$  (reduced zone scheme), or equivalently as a  $4\pi$ -periodic function  $I_{4\pi}(\phi)$  (extended zone scheme). Both representations are shown in Fig. 1, upper panels. We also include the  $2\pi$ -periodic current  $I_{2\pi}$  that results if the system can relax to its lowest energy state without constraints on the parity of  $\mathcal{N}$ .

So much for the short-junction limit. An elementary discussion of the long-junction regime (to be made rigorous in just a moment) goes as follows. For  $L \gg \xi$  we may assume [22–24] a local linear relation between the current density  $I$  and the phase gradient  $\phi/L \ll 1/\xi$ , of the form  $I = \text{const} \times ev\phi/L$ . The linear increase of  $I_-$  is interrupted

at  $\phi = 0$  by a discontinuity  $\Delta I_- = 2ev/L$ . Half of it results from the jump in the slope of the lowest occupied positive energy level  $\varepsilon = (\pi - |\phi|)\hbar v/2L$  [green arrows in Fig. 1(e)]. The jump in the slope of the highest occupied negative energy level contributes the other half. In the extended zone scheme, the resulting supercurrent  $I_{4\pi}$  is a  $4\pi$ -periodic sawtooth with a slope  $\Delta I_-/4\pi = eE_T/2\pi\hbar$ .

The corresponding parity-dependent supercurrents in the reduced zone scheme are

$$I_+ = \frac{eE_T}{2\pi\hbar} \phi, \quad I_- = \frac{eE_T}{2\pi\hbar} (\phi - 2\pi \text{sgn}\phi), \quad |\phi| < \pi. \quad (3)$$

The  $4\pi$ -periodic supercurrent  $I_{4\pi}$  switches from  $I_+$  to  $I_-$  at  $\phi = \pi$ , while  $I_{2\pi}$  remains in the branch  $I_+$  by compensating the switch in ground-state fermion parity  $\sigma$  by a switch in the parity of the electron number  $\mathcal{N}$ . These are the curves plotted in Fig. 1 (lower panels).

The maximal supercurrent is reached near  $\phi = 2\pi$  for  $I_{4\pi}$  (with parity constraint) and near  $\phi = \pi$  for  $I_{2\pi}$  (without parity constraint). There is a factor of two difference in magnitude of these critical currents in a long junction,

$$I_{4\pi,c} = eE_T/\hbar, \quad I_{2\pi,c} = eE_T/2\hbar. \quad (4)$$

In contrast, for a short junction both are the same (equal to  $e\Delta/2\hbar$ ).

To determine the crossover from the short-junction limit (2) to the long-junction limit (3), including the temperature dependence, we adapt the scattering theory of the

Josephson effect [25] to include the fermion parity constraints. Input is the scattering matrix  $s_0$  of electrons in the normal region and the Andreev reflection matrix  $r_A$  at the normal-superconductor interfaces. These take a particularly simple  $2 \times 2$  form at the quantum spin-Hall edge, but our general formulas are applicable also to *multichannel* topological superconductors.

The parity-dependent partition function is [12–14,26]

$$\begin{aligned} Z_{\pm} &= \frac{1}{2} \left( \prod_{\varepsilon>0} e^{\beta\varepsilon/2} \right) \left[ \prod_{\varepsilon>0} (1 + e^{-\beta\varepsilon}) \pm \prod_{\varepsilon>0} (1 - e^{-\beta\varepsilon}) \right] \\ &= \frac{1}{2} Z_0 \left[ 1 \pm \prod_{\varepsilon>0} \tanh(\beta\varepsilon/2) \right], \end{aligned} \quad (5)$$

with  $\beta = 1/k_B T$  and  $Z_0 = \prod_{\varepsilon>0} 2 \cosh(\beta\varepsilon/2)$  the partition function without parity constraints. From the expression for  $Z_{\pm}$  one can see that the  $\pm$  selects terms that contain an even (+) or an odd (−) number of quasiparticle excitation factors  $e^{-\beta\varepsilon}$ , as is dictated by the ground-state fermion parity. The partition function  $Z$  gives the free energy  $F$  and hence the supercurrent  $I$  [27],

$$I_{\pm} = \frac{2e}{\hbar} \frac{dF_{\pm}}{d\phi}, \quad F_{\pm} = -\beta^{-1} \ln Z_{\pm}, \quad (6)$$

$$I_{2\pi} \equiv I_0 = \frac{2e}{\hbar} \frac{dF_0}{d\phi}, \quad F_0 = -\beta^{-1} \ln Z_0. \quad (7)$$

The density of states  $\rho(\varepsilon)$  contains both the discrete spectrum for  $|\varepsilon| < \Delta$  (a sum of delta functions at the Andreev levels) and the continuous spectrum for  $|\varepsilon| > \Delta$ , including also a contribution  $\rho_S$  from the superconducting electrodes. Scattering theory gives the expression [25]

$$\rho(\varepsilon) = \text{Im} \frac{d}{d\varepsilon} \nu(\varepsilon + i0^+) + \rho_S(\varepsilon), \quad (8)$$

$$\nu(\varepsilon) = -\pi^{-1} \ln \text{Det} X(\varepsilon), \quad X = (1 - M)M^{-1/2}, \quad (9)$$

$$M(\varepsilon) = r_A^*(-\varepsilon) s_0^*(-\varepsilon) r_A(\varepsilon) s_0(\varepsilon). \quad (10)$$

The factor  $M^{-1/2}$  in the definition of  $X$ , as well as the term  $\rho_S$ , give a  $\phi$ -independent additive contribution to  $F_0$  without any effect on  $I_0$ , but we need to retain these terms here because they do enter into the parity constraint for  $I_{\pm}$ .

In the absence of parity constraints, Ref. [28] gives the free energy

$$F_0 = -\beta^{-1} \sum_{p=0}^{\infty} \ln \text{Det} X(i\omega_p), \quad (11)$$

as a sum over fermionic Matsubara frequencies  $\omega_p = (2p + 1)\pi/\beta$ . A similar calculation [29] gives the parity dependence in the form

$$\begin{aligned} F_{\sigma} &= F_0 - \beta^{-1} \ln \frac{1}{2} \left[ 1 + \sigma e^{J_S} \sqrt{\text{Det} X(0)} \right. \\ &\quad \left. \times \exp \left( \sum_{p=1}^{\infty} (-1)^p \ln \text{Det} X(i\Omega_p/2) \right) \right], \end{aligned} \quad (12)$$

$$\sigma = \text{sgn}[\text{Pf}(r_A s_0 - s_0^T r_A^T) (\text{Det} i s_0)^{-1/2}]_{\varepsilon=0}, \quad (13)$$

with bosonic Matsubara frequencies  $\Omega_p = 2p\pi/\beta$ . The ground-state fermion parity  $\sigma$  is given in terms of the Pfaffian of the antisymmetrized scattering matrix, evaluated at the Fermi energy. The sign ambiguity in the square root is resolved by fixing  $\sigma = 1$  at  $\phi = 0$ .

Equation (12) contains a contribution from the superconducting electrodes,

$$J_S = \int_{\Delta}^{\infty} d\varepsilon \rho_S(\varepsilon) \ln \tanh(\beta\varepsilon/2), \quad (14)$$

which only plays a role at temperatures  $T \gtrsim \Delta/k_B$ . The factor  $e^{J_S}$  can therefore be replaced by unity in the long-junction regime, when  $k_B T \lesssim E_T \ll \Delta$ .

We now specify these general formulas for the quantum spin-Hall edge, with the Hamiltonian [30]

$$H_{\text{BdG}} = \begin{pmatrix} v p \sigma_z + U(x) & \Delta^*(x) \sigma_y \\ \Delta(x) \sigma_y & v p \sigma_z - U(x) \end{pmatrix}. \quad (15)$$

The edge runs along the  $x$  axis,  $p = -i\hbar \partial_x$  is the momentum operator, and the electrostatic potential is  $U(x)$  (measured relative to the Fermi level). The pair potential  $\Delta(x)$  vanishes in the normal region  $|x| < L/2$ . In the two superconducting regions we set  $\Delta(x) = \Delta e^{\pm i\phi/2}$ , with a step at  $x = \pm L/2$ . This so-called ‘‘rigid boundary condition’’ is justified for a single channel coupled to a bulk superconducting reservoir [10].

A mode-matching calculation gives the scattering matrices

$$s_0 = \begin{pmatrix} 0 & e^{i\chi} \\ e^{i\chi} & 0 \end{pmatrix}, \quad \chi(\varepsilon) = \chi_0 + \varepsilon/E_T, \quad (16)$$

$$r_A = \begin{pmatrix} \alpha e^{i\phi/2} & 0 \\ 0 & -\alpha e^{-i\phi/2} \end{pmatrix}, \quad \alpha(\varepsilon) = \sqrt{1 - \frac{\varepsilon^2}{\Delta^2}} + \frac{i\varepsilon}{\Delta},$$

$$\text{Det} X(\varepsilon) = 2 \cos \phi + \alpha^2 e^{2i\varepsilon/E_T} + \alpha^{-2} e^{-2i\varepsilon/E_T}. \quad (17)$$

We discuss the various terms in these expressions. The electron scattering matrix  $s_0$  is purely off diagonal, because of the absence of backscattering along the quantum spin-Hall edge. The transmission phase  $\chi$  depends linearly on energy because of the linear dispersion. Electrostatic potential fluctuations contribute only to the energy-independent offset  $\chi_0 = -(\hbar v)^{-1} \int_0^L U dx$ , which drops out in Eq. (9). The Andreev reflection matrix  $r_A$  (from electron to hole) is unitary below the gap. Above the gap there is also propagation into the superconductor, so  $r_A$  is subunitary. The same expression (16) for  $r_A$  applies at all energies, evaluated at  $\varepsilon + i0^+$  to avoid the branch cut of the square root.

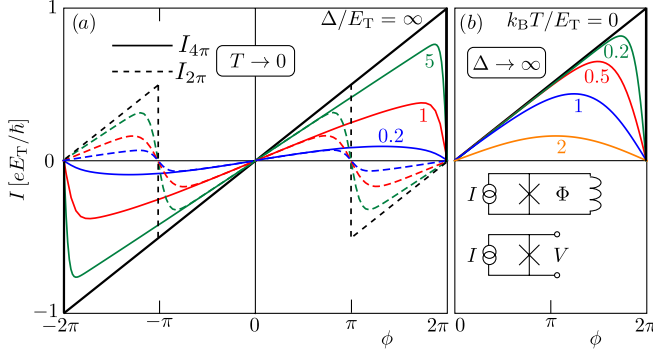


FIG. 2 (color online). Phase dependence of the parity-constrained supercurrent  $I_{4\pi}$  (solid curves, in units of  $eE_T/\hbar \propto 1/L$ ), calculated by a numerical evaluation of the Matsubara sums. The left panel shows the crossover from the short-junction to the long-junction regime in the zero-temperature limit (full interval  $-2\pi < \phi < 2\pi$ ). The right panel shows the temperature dependence in the long-junction limit (reduced interval  $0 < \phi < 2\pi$ ). The left panel also shows the supercurrent  $I_{2\pi}$  without parity constraints (dashed curves). The insets in the right panel show current-biased superconducting circuits that measure the  $I$ - $V$  and  $I$ - $\Phi$  relationships of a Josephson junction.

Putting all pieces together [29], we obtain the parity-dependent supercurrent for arbitrary ratio  $\Delta/E_T$ . In the short-junction limit  $\Delta/E_T \rightarrow 0$  we recover the known result (2), when the energy dependence of the scattering matrix and the phase sensitivity of the continuous spectrum can both be ignored. In the opposite long-junction limit  $\Delta/E_T \rightarrow \infty$  we find

$$I_{4\pi} = I_0 - \frac{2e}{\hbar\beta} \frac{d}{d\phi} \ln \left[ \frac{1}{2} + \cos(\phi/2) e^{S-\pi/2\beta E_T} \right], \quad (18)$$

$$S = \sum_{p=1}^{\infty} (-1)^p \ln(1 + 2e^{-\Omega_p/E_T} \cos \phi + e^{-2\Omega_p/E_T}), \quad (19)$$

$$I_{2\pi} \equiv I_0 = \frac{2e}{\hbar\beta} \sin \phi \sum_{p=0}^{\infty} [\cos \phi + \cosh(2\omega_p/E_T)]^{-1}. \quad (20)$$

The plot of the results in Fig. 2 shows that the crossover from a sine to a sawtooth shape occurs early: already for  $\Delta = E_T$  (so for  $L = \xi$ ) the maximum of the current-phase relationship is close to  $\phi = 2\pi$ . The sawtooth shape is preserved with increasing temperature for  $k_B T \lesssim \frac{1}{2} E_T$ .

These are encouraging results for the experimental accessibility of the long-junction regime. The quantum spin-Hall effect has been observed in HgTe/CdTe quantum wells [31], and more recently in InAs/GaSb quantum wells [32]—where also Andreev reflection from superconducting Nb electrodes was demonstrated [33]. For a typical Fermi velocity of  $v \approx 10^5$  m/s in a semiconductor and superconducting gap  $\Delta \approx 1$  meV in bulk Nb, the coherence length is  $\xi = 70$  nm, so the Josephson junction length  $L = 0.5 \mu\text{m}$  from Ref. [33] is deep in the long-junction

regime. Since the long-junction regime is already entered for  $L \approx \xi$ , this would apply even if the effective superconducting gap is well below the bulk value of Nb. The corresponding Thouless energy is  $E_T/k_B = 1.5$  K, so at  $T = 100$  mK one should be close to the low-temperature limit.

In the ongoing search for the  $4\pi$ -periodic Josephson effect the first results have been reported [34] for the ac effect (fractional Shapiro steps [9,15–18]). A dc measurement of the current-flux ( $I$ - $\Phi$ ,  $\phi = 2e\Phi/\hbar$ ) relationship, for times large compared to the time  $\tau_{\text{qp}} \approx \mu\text{s}$  for unpaired quasiparticles to tunnel into the system [35], will measure the  $2\pi$  periodic  $I_{2\pi}$  rather than  $I_{4\pi}$ . Such a phase-sensitive measurement (Fig. 2, upper inset) would produce the critical current  $I_{2\pi,c}$  without any signature of the parity anomaly. In contrast, a phase-insensitive measurement of the critical current through the current-voltage ( $I$ - $V$ ) characteristic (lower inset) will produce  $I_{4\pi,c}$  even on time scales  $\gg \tau_{\text{qp}}$ , because the phase of a resistively shunted (overdamped) circuit can adjust to a change in  $\mathcal{N}$  on time scales much smaller than  $\tau_{\text{qp}}$ . A change in the parity of  $\mathcal{N}$  will be compensated by a  $2\pi$  phase shift, without a change in critical current [29]. In a short junction,  $I_{2\pi,c}$  and  $I_{4\pi,c}$  are the same, so this does not help, but in a long junction they differ by up to a factor of two.

In conclusion, we have presented a theory for the  $4\pi$ -periodic Josephson effect on large scales compared to the superconducting coherence length. A multitude of subgap states, as well as a continuum of states above the gap, contribute to the supercurrent for  $L \gg \xi$ , but still the parity anomaly responsible for the  $4\pi$  periodicity persists. In fact, we have found that in a long junction the anomaly manifests itself also in a phase-insensitive way, through a doubling of the critical current. This opens up new possibilities for the detection of this topological effect at the quantum spin-Hall edge [31–33], and possibly also in semiconductor nanowires [34,36–41].

Discussions with A.R. Akhmerov are gratefully acknowledged. This research was supported by the Dutch Science Foundation NWO/FOM and by an ERC Advanced Investigator grant.

- [1] M. Ma and A. Yu. Zyuzin, *Europhys. Lett.* **21**, 941 (1993).
- [2] J.A.M. van Ostaay, A.R. Akhmerov, and C.W.J. Beenakker, *Phys. Rev. B* **83**, 195441 (2011).
- [3] M. Stone and Y. Lin, *Phys. Rev. B* **83**, 224501 (2011).
- [4] P. Rickhaus, M. Weiss, L. Marot, and C. Schönenberger, *Nano Lett.* **12**, 1942 (2012).
- [5] M. Popinciuc, V.E. Calado, X.L. Liu, A.R. Akhmerov, T.M. Klapwijk, and L.M.K. Vandersypen, *Phys. Rev. B* **85**, 205404 (2012).
- [6] K. Komatsu, C. Li, S. Autier-Laurent, H. Bouchiat, and S. Guéron, *Phys. Rev. B* **86**, 115412 (2012).
- [7] L. Fu and C.L. Kane, *Phys. Rev. B* **79**, 161408(R) (2009).
- [8] A. Yu. Kitaev, *Phys. Usp.* **44**, 131 (2001).

- [9] H.-J. Kwon, K. Sengupta, and V.M. Yakovenko, *Braz. J. Phys.* **33**, 653 (2003); *Eur. Phys. J. B* **37**, 349 (2004).
- [10] A. A. Golubov, M. Y. Kupriyanov, and E. Il'ichev, *Rev. Mod. Phys.* **76**, 411 (2004).
- [11] R. M. Lutchyn, J. D. Sau, and S. D. Sarma, *Phys. Rev. Lett.* **105**, 077001 (2010).
- [12] K. T. Law and P. A. Lee, *Phys. Rev. B* **84**, 081304 (2011).
- [13] P. A. Iosevich and M. V. Feigel'man, *Phys. Rev. Lett.* **106**, 077003 (2011).
- [14] F. S. Nogueira and I. Eremin, *J. Phys. Condens. Matter* **24**, 325701 (2012).
- [15] D. M. Badiane, M. Houzet, and J. S. Meyer, *Phys. Rev. Lett.* **107**, 177002 (2011).
- [16] P. San-Jose, E. Prada, and R. Aguado, *Phys. Rev. Lett.* **108**, 257001 (2012).
- [17] F. Domínguez, F. Hassler, and G. Platero, *Phys. Rev. B* **86**, 140503(R) (2012).
- [18] D. I. Pikulin and Yu. V. Nazarov, *Phys. Rev. B* **86**, 140504 (R) (2012).
- [19] M. König, H. Buhmann, L. W. Molenkamp, T. Hughes, C.-X. Liu, X.-L. Qi, and S.-C. Zhang, *J. Phys. Soc. Jpn.* **77**, 031007 (2008).
- [20] C. W. J. Beenakker and H. van Houten, *Phys. Rev. Lett.* **66**, 3056 (1991); Extended version at [arXiv:cond-mat/0512610](https://arxiv.org/abs/cond-mat/0512610).
- [21] It is a pervasive misunderstanding that the factor  $g = 2$  in the relation (1) between supercurrent and Andreev levels accounts for the charge  $2e$  of the Cooper pairs, rather than counting the spin degeneracy. Because of this misunderstanding, the results for the supercurrent carried by Majorana zero modes (which have  $g = 1$ ) should be divided by two in Ref. [9] and many follow-up papers. The origin of the misunderstanding is discussed in more detail by N. M. Chtchelkatchev and Yu. V. Nazarov, *Phys. Rev. Lett.* **90**, 226806 (2003).
- [22] C. Ishii, *Prog. Theor. Phys.* **44**, 1525 (1970).
- [23] J. Bardeen and J. L. Johnson, *Phys. Rev. B* **5**, 72 (1972).
- [24] A. V. Svidzinsky, T. N. Antsygina, and E. N. Bratus, *J. Low Temp. Phys.* **10**, 131 (1973).
- [25] C. W. J. Beenakker, *Phys. Rev. Lett.* **67**, 3836 (1991); Extended version at [arXiv:cond-mat/0406127](https://arxiv.org/abs/cond-mat/0406127).
- [26] M. T. Tuominen, J. M. Hergenrother, T. S. Tighe, and M. Tinkham, *Phys. Rev. Lett.* **69**, 1997 (1992).
- [27] The factor of two in the relation (6) between supercurrent and free energy accounts for the Cooper pair charge, with all degeneracies included in the partition function. Please see Ref. [21] to avoid any misunderstanding.
- [28] P. W. Brouwer and C. W. J. Beenakker, *Chaos, Solitons Fractals* **8**, 1249 (1997). Several misprints are corrected in the online version at [arXiv:cond-mat/9611162](https://arxiv.org/abs/cond-mat/9611162).
- [29] See Supplemental Material at <http://link.aps.org/supplemental/10.1103/PhysRevLett.110.017003> for details of the calculations.
- [30] The basis chosen for the Bogoliubov–de Gennes Hamiltonian (15) is {spin-up electron, spin-down electron, spin-up hole, spin-down hole}. In this basis, the electron and hole blocks of  $H_{\text{BdG}}$  are minus each others complex conjugate and the electron and hole scattering matrices  $s_{ee}$ ,  $s_{hh}$  are related by  $s_{hh}^*(-\varepsilon) = s_{ee}(\varepsilon) \equiv s_0(\varepsilon)$ . Similarly, the Andreev reflection matrices  $s_{he}$ ,  $s_{eh}$  from electron to hole and from hole to electron are related by  $s_{eh}^*(-\varepsilon) = s_{he}(\varepsilon) \equiv r_A(\varepsilon)$ .
- [31] M. König, S. Wiedmann, C. Brüne, A. Roth, H. Buhmann, L. W. Molenkamp, X.-L. Qi, and S.-C. Zhang, *Science* **318**, 766 (2007).
- [32] I. Knez, R.-R. Du, and G. Sullivan, *Phys. Rev. Lett.* **107**, 136603 (2011).
- [33] I. Knez, R.-R. Du, and G. Sullivan, *Phys. Rev. Lett.* **109**, 186603 (2012).
- [34] L. P. Rokhinson, X. Liu, and J. K. Furdyna, *Nat. Phys.* **8**, 795 (2012).
- [35] D. Rainis and D. Loss, *Phys. Rev. B* **85**, 174533 (2012).
- [36] V. Mourik, K. Zuo, S. M. Frolov, S. R. Plissard, E. P. A. M. Bakkers, and L. P. Kouwenhoven, *Science* **336**, 1003 (2012).
- [37] M. T. Deng, C. L. Yu, G. Y. Huang, M. Larsson, P. Caroff, and H. Q. Xu, *Nano Lett.* **12**, 6414 (2012).
- [38] A. Das, Y. Ronen, Y. Most, Y. Oreg, M. Heiblum, and H. Shtrikman, *Nat. Phys.* **8**, 887 (2012).
- [39] S. Ryu, A. Schnyder, A. Furusaki, and A. Ludwig, *New J. Phys.* **12**, 065010 (2010).
- [40] A. R. Akhmerov, J. P. Dahlhaus, F. Hassler, M. Wimmer, and C. W. J. Beenakker, *Phys. Rev. Lett.* **106**, 057001 (2011).
- [41] M. Diez, J. P. Dahlhaus, M. Wimmer, and C. W. J. Beenakker, *Phys. Rev. B* **86**, 094501 (2012).